Research Square

Preprints are preliminary reports that have not undergone peer review.
They should not be considered conclusive, used to inform clinical practice,
or referenced by the media as validated information.

A stable catalyst for simultaneous catalytic removal of nitrogen oxide and toluene at low temperature

Yu Yan
Shanghai University
Linmin Lao
Shanghai University
Chengyan Li
Nanjing Institute of Environmental Sciences
Yang Yue
Shanghai University
Guangren Qian
MGI of Shanghai University
Jia Zhang
irujam@t.shu.edu.cn

Shanghai University

Research Article

Keywords: Catalytic oxidation, Catalytic reduction, Volatile organic compounds, Nitrogen oxide, Titanium dioxide

Posted Date: March 30th, 2026

DOI: https://doi.org/10.21203/rs.3.rs-9218535/v1

License: This work is licensed under a Creative Commons Attribution 4.0 International License. Read Full License

Additional Declarations: No competing interests reported.

Abstract

Simultaneous catalytic removal of nitrogen oxide and volatile organic compounds at low temperature is a challenge since these two pollutants have a competitive effect for the catalytic active site. This work has compared the different behaviors of V/TiO_2 and CeV/TiO_2 in separate and simultaneous catalytic removal of NO and toluene. Both the catalysts have been detailly characterized and compared. The catalytic oxidation of toluene obviously disturbed the catalytic reduction of NO by V/TiO_2. NO removal was decreased from 99% to 72% at 250°C. In comparison, the toluene only decreased the NO removal of CeV/TiO_2 from 95% to 85%. From the viewpoint of toluene, the NO slightly decreased the toluene removal of V/TiO_2 but hardly affected the toluene removal of CeV/TiO_2. The more stable performance of CeV/TiO_2 was attributed to its lower adsorption energies/abilities for various pollutants and derived intermediates.

Article Highlights

(1) Catalytic oxidation and reduction have a mutual interference.

(2) CeV/TiO_2 is more stable than V/TiO_2 in the mutual interference.

(3) The stability is attributed to lower adsorption energies for various pollutants.

1. Introduction

Volatile organic compounds (VOCs) and nitrogen oxide (NOx) are two typical air pollutants [1]. Examples of VOCs are halogenated hydrocarbons, aldehydes, aromatics, alkanes, ketones, and sulfur containing compounds. High concentrations of these VOCs cause irritations, dizziness, headaches, and even cancers for both humans and animals [2]. NOx potentially cause acid rain, photochemical smog, and eutrophication. Furthermore, VOCs and NOx are both crucial precursors of ozone and $PM_{2.5}$ [3]. Some industries only discharge VOCs, such as petrochemical, pharmaceutical, paint, and leather manufacturing. However, some others discharge both VOCs and NOx, such as thermal power, incineration, glass, cement, steel sintering, and ceramics. Therefore, the simultaneous removal of VOCs and NOx is a necessary.

If only VOCs are aimed to be removed, the catalytic oxidation is accepted to be the most effective and reliable technology. Theoretically, VOCs react with O_2 to form H_2O and CO_2 with the help of the catalyst [4]. The commercial VOCs catalyst includes noble-metal (Pt, Pd, Ag) and transition-metal (Mn, Ce, Cu) catalysts [5, 6]. If the polluted gas only contains NOx, selective catalytic reduction (SCR) is widely recognized as the most cost-effective method [7]. In brief, NOx catalytically react with the reductant, forming harmless H_2O and

N_2 [8]. The most typical reductant and catalyst are NH_3 and V/TiO_2, respectively. In fact, V/TiO_2 is a commercial catalyst used in the real industry [9]. In recent years, other reductant is put forward to replace NH_3, such as hydrocarbons and carbon monoxide [10, 11]. Thus, researchers also ask themselves if VOCs can potentially be used as the reductant of SCR.

The simultaneous removal thus reduces equipment construction costs and space requirement [12]. However, two difficulties exists. On one hand, one bifunctional catalyst must be developed working at a same temperature range for both these two gases [13]. This is relatively easy to solve since typical catalytic temperatures for these gases are 180–300°C. We even can find catalysts that can efficiently catalyze these gases alone. For example, MnO_2 effectively catalyze VOCs and NOx at 250°C and 100–250°C, respectively [14, 15]. On the other hand, catalytic oxidation and catalytic reduction potentially affect each other because these two processes both utilizes surface oxygens on the catalyst [16, 17]. Several attempts have showed that the NH_3-SCR inhibits the toluene oxidation if a same catalyst is used [18, 19]. The main reason is that the reactive intermediate of one catalyst is a blocking species for the other [19]. Therefore, decreasing the competitive effect seems to be more pragmatic than using VOCs as the reductant of SCR.

In this work, V/TiO_2 and CeV/TiO_2 are synthesized and compared in simultaneous catalytic removal of toluene and NO. Both the catalysts and catalytic processes are detailly characterized. The adsorption energies of different gaseous molecules are calculated by the density functional theory. With these investigations, a mechanism is put forward to explain why CeV/TiO_2 is a more stable catalyst.

2. Materials and Methods

2.1. Catalyst Preparations

The catalyst was synthesized by an impregnation method [20]. In detail, ammonium metavanadate and ammonium cerium nitrate were dissolved in 100 mL of deionized water at 70°C. TiO_2 (5 g) was dispersed into the above solution, and stirred for 2 h. After a well mixing, the solution was dried at 105°C before being calcined at 450°C for 2 h. The prepared catalysts were milled to 50 mesh and denoted as V/Ti and CeV/Ti. The metal contents of these catalysts were detected by which were an Inductively Coupled Plasma-Atomic Emission Spectrometry (IRIS Advantage 1000, Thermo Fisher) after the standard digestion. V/Ti resulted in a V-loading amount of 5 wt.%. In CeV/Ti, molar ratio between Ce and V was around 1:1.

2.2. Catalytic Performances

Catalytic oxidation of toluene and NH_3-SCR were carried out on a fixed-bed reactor [21], which is showed in **Fig. S1** in the Supporting Information. Setup details are also provided below the figure. Removals of toluene (X_T) and NO (X_{NO}) are calculated according to Eqs. (1) and (2). N_2 selectivity is calculated accordingly by Eq. (3). In these equations, the subscripts “in” and “out” stands for concentrations in the inflow and outflow, respectively.

$$\text{Toluene removal } (X_T, \%) = \left(\frac{[\text{Toluene}]_{in} - [\text{Toluene}]_{out}}{[\text{Toluene}]_{in}}\right) \times 100\% \quad (1)$$

$$\text{NO removal } (X_{NO}, \%) = \left(\frac{[NO]_{in} - [NO]_{out}}{[NO]_{in}}\right) \times 100\% \quad (2)$$

$$N_2 \text{ selectivity } (\%) = \left(1 - \frac{2N_2O_{out}}{NO_{x_{in}} - NO_{x_{out}} + NH_{3_{in}} - NH_{3_{out}}}\right) \times 100 \quad (3)$$

2.3. Characterizations

X-ray diffraction (XRD) was carried out using a powder diffractometer (MiniFlex600, Rigaku) equipped with Cu Kα radiation. Textural properties were detected by Autosorb-IQ2. Temperature-programmed desorption of NH_3 (NH_3-TPD) and temperature-programmed reduction of H_2 (H_2-TPR) were carried on a VD Sorb-91i (Quzhou Vodo instrument Co. Ltd., China). Binding energies of elements were analyzed by a K-Alpha X-ray photoelectron spectroscopy (XPS, Thermo Scientific, USA). *In-situ* Diffuse Reflection Fourier Transform Infrared Spectrometer (DRIFTs) was carried out on Nicolet IS10 (Thermo Scientific) with an MCT detector at a resolution of 4 cm^{-1} [22]. The sampling intervals are all 0, 1, 3, 5, 10, 20, and 30 min. All calculations were based on spin polarization density functional theory (DFT) such as Vienna First Principles (VASP) and projected Enhanced waves (PAW). The exchange correlation function used was a local density approximation with generalized gradient correction, called GGA-PBE [23, 24]. The energy of the plane wave was truncated to 400 eV for all atoms, and the ion positions of all structures were relaxed until the force converges to 0.03eV·Å.

3. Results and Discussion

3.1. Simultaneous Catalytic Removal of NO and Toluene

Figure S2A investigates the possibility of using toluene as the reductant of SCR process. Unfortunately, the NO removals are close to zero at the tested temperatures. If the O_2 is

removed from the inflow gas, both the conversions of NO and toluene are close to zero (**Fig. S2B**). However, if the temperature is further increased to 350°C, both NO and toluene conversions are increased to about $20-30\%$. Considering this, even the toluene is feasible to be used as the reductant of SCR, the suitable temperature is too high.

On one hand, if V/TiO_2 is used in the SCR, a removal of 65% is reached at 100°C (Fig. 1A). When the temperature is increased to 200°C, the removal has been increased to 99%. In comparison, when the toluene is mixed into the inflow gas, the NO removal is obviously decreased. For example, the removal is decreased to 37% at 100°C. On the other hand, if V/TiO_2 is used in the catalytic oxidization of toluene, the ignition temperature is started between 200 and 250°C (Fig. 1B). When the NO and NH_3 are mixed into the inflow gas, the toluene removal is also affected. For example, the removal at 300°C is decreased from 99% to 67%.

When Ce is co-doped onto the TiO_2, CeV/TiO_2 has a better resistant ability for co-existing toluene (Fig. 1A). The removals between 100 and 200°C is hardly affected. The removal is decreased from 98% to 86% at 300°C. The difference is 12%. In comparison, the difference is 23% using V/TiO_2. As for the side of toluene, similar phenomenon is observed (Fig. 1B). The catalytic activity of CeV/TiO_2 is hardly affected by the co-existing NO and NH_3. The conversion curves are almost overlapped. In addition, the co-catalysis has no influence on the N_2 selectivity either (**Fig. S2C**). After all, CeV/TiO_2 is more stable than V/TiO_2 in the simultaneous catalysis.

3.2. Basic Characterizations

Table 1
Textural properties of V/TiO_2 and CeV/TiO_2.

Specific surface area ($m^2 \cdot g^{-1}$)	**V/TiO_2**	**CeV/TiO_2**
	47.2	**48.5**
Pore volume ($cm^3 \cdot g^{-1}$)	0.42	0.43
Pore size (nm)	38.3	38.8
O_α (%)	87	86
O_β (%)	8	8
O_γ (%)	5	6
V^{3+} (%)	26	12
V^{4+} (%)	44	53
V^{5+} (%)	30	35

V/TiO_2 and CeV/TiO_2 show a similar XRD pattern (Fig. 2A). Anatase TiO_2 (PDF#84-1285) has diffractions at 25.3 ° (101), 37.8 ° (004), 48.0 ° (200), 53.9 ° (105), 55.1 ° (211), and 62.7 ° (204), while the main diffraction of rutile TiO_2 (PDF#87–0710) is detected 27.5 ° (110) [25]. Besides, both catalysts exhibits a type IV isotherm with a hysteresis loop (Fig. 2B), which is the proof of the mesoporous structure [26]. In fact, the two catalysts have similar textural properties (Table 1). For example, the specific surface areas are 47.2 and 48.5 $m^2 \cdot g^{-1}$.

Brønsted-acidic sites (100–250°C) and the Lewis-acidic sites (300–450°C) are observed in **Fig. S3A**. The Brønsted-acid site favors the SCR [27]. After the integration, the relative area of the Brønsted-acidic site in V/TiO_2 is 283 (a.u.), which the relative area of the Lewis-acid site is 96 (a.u.). In comparison, CeV/TiO_2 has 148 (a.u.) of Brønsted-acidic sites and 169 (a.u.) of Lewis-acid sites. This explains why V/TiO_2 has a better SCR activity than CeV/TiO_2. H_2-TPR stands for the reduction of both VOx and CeOx (**Fig. S3B**). The overall reductive ability is reduced after co-doping Ce in V/TiO_2.

The peak of XPS O 1s at 528–534 eV is typically made up to lattice oxygen (O_α), oxygen vacancy (O_β), and surface hydroxyl (O_γ) [20]. Figure 2C are fitted into these components and the results are listed in Table 1. V/TiO_2 and CeV/TiO_2 show similar amounts of these oxygen species. Their main components are O_α, which occupies 86–87% of all oxygen species. Figure 2D further compares the XPS V 2p of these two catalysts. The V 2p is

usually fitted into three species, including V^{5+} (517 eV), V^{4+}(516 eV), and V^{3+} (515 eV) [26]. Between the two catalysts, V/TiO_2 exhibits a higher proportion of low-valence V species (70%), which enhances the redox cycle on the catalyst surface [28]. This is consistent with the H_2-TPR result.

According to the above comparisons, the reason is revealed why V/TiO_2 has better catalytic performances than CeV/TiO_2 in separate removal of toluene and NO. However, the above similarity and differentia is infeasible to explain why CeV/TiO_2 has a more stable performance in simultaneous removal of toluene and NO.

3.3. Catalytic Processes

When the catalytic oxidation occurs on CeV/TiO_2 at 250°C (Fig. 3A), several obvious peaks are observed at 3029, 2930, 1644, and 1513 cm^{-1}. According to previous reports, clear bands at 1513and 1644 cm^{-1} are associated with the vibration of aromatic rings [29]. 2931 cm^{-1} is attributed to the antisymmetric peaks of CH in CH_2, i.e., the benzyl radicals are generated [30]. 3029 cm^{-1} is derived from C−H stretching vibration in benzene ring [30]. After NH_3 flows into the reactor, the peaks are hardly affected at 1513 and 1644 cm^{-1}. However, new peaks are observed at 1451 and 1173 cm^{-1}, which are attributed to adsorbed NH_3 species on Brønsted and Lewis acid sites, respectively [31]. At the same time, the peaks at 3029 and 2930 cm^{-1} are placed by new peaks at 3250 and 3151 cm^{-1} step by step. They belongs to ascribed to N–H stretching vibration modes of NH_3 and NH_4^+, respectively [32, 33]. This indicates that two possibilities. One is that intermediates of toluene decomposition are replaced by NH_3-derived species. The other is that these intermediates even react with NH_3. Whatever the possibility, NH_3-derived species are feasible to be adsorbed onto the catalyst surface. After $NO + O_2$ flows into the reactor, the peaks at 1513 and 1644 cm^{-1} still exists even after 30 min. On the contrary, the intensities of NH_3-derived species are all decreased along with time. This indicates that NH_3 molecules are first adsorbed on the catalyst surface and then react with NO, which is called an Eley-Rideal (E-R) mechanism.

In comparison, when V/TiO_2 is used in the catalytic oxidation of toluene (Fig. 3B), the peak at 1400 cm^{-1} represents the shorter carboxylate species (especially acetate) [34]. In addition, peaks are also observed at 3029, 2930, 1644, and 1513 cm^{-1}. After NH_3 flows into the reactor, above peaks are hardly affected. Although the peaks at 3029 and 2930 cm^{-1} are obviously decreased, no NH_3-derived species are formed. After $NO + O_2$ flows into the reactor, the relative intensities at 1644 and 1513 cm^{-1} are decreased. The peak intensity at 1400 cm^{-1} is stable. Thus, the intermediate shorter carboxylate species is

hard to be replaced. After all, no $NO + O_2$ derived species are formed. In other words, the intermediates of toluene decomposition disturb the SCR on V/TiO_2. This is different from CeV/TiO_2, which functions normally in SCR even with the intermediates.

In Fig. 4A, $NO + O_2$ flows into the reactor after the catalytic oxidation of toluene for 30 min. The peaks at 3029 and 2930 cm^{-1} removed from the catalyst surface by the $NO + O_2$ flow. An overlapping peak at 1538 cm^{-1} is formed and attributed to NO_2 on Lewis acid sides. After NH_3 flows into the reactor, these peaks are hardly affected). Besides, peaks are formed at 3250 and 3151 cm^{-1}. These phenomena at least suggest that NH_3 are adsorbed. As is well-known, if NH_3 reacts with the pre-adsorbed $NO + O_2$, the SCR is carried out by the Langmuir-Hinshelwood (L-H mechanism). However, it is hard to judge whether SCR is carried out by this mechanism.

After $NO + O_2$ flows into the reactor (Fig. 4B), the peak intensities are decreased at 1644, and 1513 cm^{-1}. However, the three peaks still observed after 30 min. Although the peak intensities are also decreased at 3029 and 2930 cm^{-1}, no obvious $NO + O_2$-derived species are recognized. Similarly, after NH_3 flows into the reactor, no further change is observed. According to the previous reports, the V/TiO_2-based catalyst participates in the SCR by both L-H and E-R mechanisms [35, 36]. Considering this, the catalytic oxidation of toluene interferes the L-H mechanism by both the catalysts but only interferes the E-R mechanism by V/TiO_2. This is the reason why CeV/TiO_2 is more stable than V/TiO_2 in the simultaneous catalysis of toluene and NO.

3.4. Catalytic Mechanism

Table 2
Adsorption energies of different gases on V/TiO_2 and CeV/TiO_2.

CO_2 adsorption	**V/TiO_2**	**CeV/TiO_2**
	4.127	**2.885**
NH_3 adsorption	-1.693	-1.688
NO adsorption	11.572	4.441
NO_2 adsorption	-0.959	-0.841

DFT calculations are used to compare the adsorption energies of different gases (including CO_2, NH_3, NO, and NO_2) on V/TiO_2 (**Fig. S4A**) and CeV/TiO_2 (**Fig. S4B**). The detailed values are listed in Table 2. A negative adsorption energy indicates a spontaneous adsorption on the surface. Besides, the more negative the adsorption energy, the stronger

the adsorption [37]. Therefore, both NH_3 and NO_2 can be adsorbed spontaneously by both V/TiO_2 and CeV/TiO_2. However, V/TiO_2 has a stronger adsorption than CeV/TiO_2 since its adsorption energies are more negative. On the contrary, a positive value indicates that the adsorption process is endothermic [38]. Therefore, the adsorption energy of CO_2 is significantly decreased from 4.127 eV (V/TiO_2) to 2.885 eV (CeV/TiO_2). CO_2 is an important intermediate of toluene decomposition. Its release from the catalyst surface is determining to the continuous catalysis. A lower adsorption energy indicates that the molecule is easier to be replaced by other gases. Similarly, the adsorption energy of NO is significantly decreased from 11.572 eV (V/TiO_2) to 4.441 eV (CeV/TiO_2).

A more stable simultaneous catalysis of toluene and NO is attributed to lower adsorption energies on the catalyst surface after co-doping Ce. When the toluene are adsorbed by V/TiO_2 and CeV/TiO_2. Intermediates are formed on the surfaces (**Fig. S4CI**). On one hand, NH_3 is feasible to replace these intermediates on the CeV/TiO_2 but infeasible to replace those on the V/TiO_2 (**Fig. S4CII**). As a result, NOx can react with the NH_3-dervied species to complete the E-R mechanism on CeV/TiO_2 (**Fig. S4CIII** and **3**). On the other hand, NO is infeasible to replace the intermediates on V/TiO_2 and CeV/TiO_2 (**Fig. S4CIV**). As a result, the L-H mechanism is hindered on both these catalysts (Fig. 4).

4. Conclusion

In this work, V/TiO_2 and CeV/TiO_2 were synthesized and compared in simultaneous SCR and catalytic oxidation of toluene. CeV/TiO_2 was more stable than V/TiO_2 in the simultaneous catalysis. The reason was revealed that CeV/TiO_2 had weaker adsorption abilities for various pollutants and derived intermediates. These species are easier to be replaced by each other on the catalyst surface. Therefore, this work put forward a successful example of designing a suitable catalyst instead of a merely active one.

Declarations

Acknowledgements

We appreciate the help of the Instrumental Analysis & Research Center of Shanghai University in sample characterization.

Funding

This project was financially supported by the Natural Science Foundation of Shanghai 2021 Science and Technology Innovation Action Plan (21ZR1424000).

Author Information

Authors and Affiliations

Yu Yan,[1] Linmin Lao,[1] Chengyan Li,[2] Yang Yue,[1,3] Guangren Qian,[3] Jia Zhang [1,3]

[1] SHU Center of Green Urban Mining & Industry Ecology, School of Environmental and Chemical Engineering, Shanghai University, No. 381 Nanchen Road, Shanghai 200444, P. R. China

[2] Nanjing Institute of Environmental Sciences, Ministry of Ecology and Environment of the People's Republic of China, Nanjing 210042, China

[3] MGI of Shanghai University, Xiapu Town, Xiangdong District, Pingxiang City, Jiangxi, 337022, P. R. China;

Contributions

Yu Yanand **Linmin Lao**contributes to experiment design, data acquisition and analysis, and manuscript drafting. **Chengyan Li** and **Yang Yue** contribute to characterizations. **Guangren Qian** contributes to resources. **Jia Zhang** contributes to interpretation of data and critical revision of the manuscript.

Corresponding Author

Correspondence to Jia Zhang.

Ethics Declarations

Ethics Approval and Consent to Participate

Not applicable.

Consent for Publication

Not applicable.

Competing Interests

The authors have no relevant financial or non-financial interests to disclose.

Supporting Information

Supplementary data Supplementary data to this article can be found online.

References

1. Liang J, Hang J, Jia S et al (2025) O_3–NOx–VOCs photochemical pollutant dispersion in 2D street canyon under effects of solar radiation. Atmos Environ 344:121032
2. Cheng L, Lei J, Ren X et al (2025) Trace lanthanum-modified α-MnO_2 catalyst for total oxidation of toluene by weakening the Mn–O bond. React Kinet Mech Catal 138:3813–3829
3. Tao C, Zhang Q, Huo S et al (2024) PM2.5 pollution modulates the response of ozone formation to VOC emitted from various sources: Insights from machine learning. Sci Total Environ 916:170009
4. Jiang Z, Wang Y, Chen C et al (2024) Progress and challenge of functional single-atom catalysts for the catalytic oxidation of volatile organic compounds. Chin Chem Lett 35:109400
5. Bai H, Wang Z, Zhang J et al (2021) Synthesis of a perovskite-type catalyst from Cr electroplating sludge for effective catalytic oxidization of VOC. J Environ Manage 294:113025
6. Tong W, Yang J, Ji Y et al (2026) Unraveling the role of oxygen species in Pt/MnO_2 catalysts for low-temperature HCHO abatement: A precursor-dependent study. J Taiwan Inst Chem Eng 181:106541
7. Elkaee S, Phule AD, Yang JH (2024) Advancements in (SCR) technologies for NOx reduction: A comprehensive review of reducing agents. Process Saf Environ Prot 184:854–880
8. Chen S, Lv Y, Hong J et al (2023) Recognizing the formation of single-atom vanadium by enthalpy and its advantage in selective catalytic reduction of nitrogen oxide. Process Saf Environ Prot 175:111–118
9. Zhao L, Yu Y-f, Wang H-w et al (2025) Insights into the effect of Cd on simultaneous removal of NO_x and dioxins over V_2O_5-MoO_3/TiO_2 catalyst: A combination of experimental and DFT study. Sep Purif Technol 357:130159
10. Huang W, Yang S, Li X et al (2024) Performance, reaction mechanism and modification methods for Mn-based CO-SCR catalysts: A review. J Environ Chem Eng 12:113593
11. Zhao H, Meng P, Gao S et al (2024) Recent advances in simultaneous removal of NOx and VOCs over bifunctional catalysts via SCR and oxidation reaction. Sci Total Environ 906:167553
12. Zhou X, Xie J, Zhang R et al (2024) Recent advances in different catalysts for synergistic removal of NOx and VOCs: A minor review. J Environ Chem Eng 12:111764
13. Ji H, Hou Y, Li B et al (2024) Insight into the mechanism of simultaneous removal of NOx and toluene by MnCuTi ternary catalyst. Mol Catal 559:114110

14. Lu T, Zhang C, Du F et al (2023) Mutual inhibition effects on the synchronous conversion of benzene, toluene, and xylene over MnOx catalysts. J Colloid Interface Sci 641:791–802
15. Xu S, Chen J, Li Z et al (2023) Highly ordered mesoporous MnOx catalyst for the NH_3-SCR of NOx at low temperatures. Appl Catal A 649:118966
16. Mao H, Xu M, Li S et al (2023) Accelerating surface lattice oxygen activation of Pt/TiO_{2-x} by modulating the interface electron interaction for efficient photocatalytic toluene oxidation. ACS ES&T Eng 3:1851–1863
17. Zheng Y, Fu K, Yu Z et al (2022) Oxygen vacancies in a catalyst for VOCs oxidation: synthesis, characterization, and catalytic effects. J Mater Chem A 10:14171–14186
18. Li Z, Gao Y, Wang Q (2022) The influencing mechanism of NH_3 and NOx addition on the catalytic oxidation of toluene over $Mn_2Cu_1Al_1O_x$ catalyst. J Clean Prod 348:131152
19. Ye L, Lu P, Peng Y et al (2021) Impact of NOx and NH_3 addition on toluene oxidation over MnOx-CeO_2 catalyst. J Hazard Mater 416:125939
20. Chen W, Chen S, Song M et al (2024) Enthalpy change of V–Ti interface as an indicator of high catalytic activity. Inorg Chem 63:19266–19276
21. Zeng J, Yue Y, Gao Q et al (2019) Co-treatment of hazardous wastes by the thermal plasma to produce an effective catalyst. J Clean Prod 208:243–251
22. Hao C, Zhang C, Zhang J et al (2022) An efficient strategy to screen an effective catalyst for NOx-SCR by deducing surface species using DRIFTS. J Colloid Interface Sci 606:677–687
23. Kresse F (1996) Efficient iterative schemes for ab initio total-energy calculations using a plane-wave basis set. Phys. Rev. B
24. Perdew B (1996) Wang Generalized gradient approximation for the exchange-correlation hole of a many-electron system. Phys. Rev. B
25. Chen W, Lao L, Zhang Y et al (2025) Producing a monolithic catalyst for the catalytic oxidization of dioxins by comparing extrusion and coating methods. React Kinet Mech Catal 138:791–803
26. Nguyen T-B, Hwang M-J, Ryu K-S (2012) High adsorption capacity of V-doped TiO_2 for decolorization of methylene blue. Appl Surf Sci 258:7299–7305
27. Chu X, Yang L, Feng D et al (2024) Performance of titanium-based catalysts loaded with transition metals (Cu, Mn and Fe) for simultaneous elimination of NO and typical VOCs. Catal Lett 154:2255–2264
28. Xu Y, Wu X, Cao L et al (2019) Crystal orientation-dependent activity of tungsten-based catalysts for selective catalytic reduction of NOx with NH_3. J Catal 375:294–303
29. Suárez-Vázquez SI, Moreno-Román EJ, Zanella R et al (2022) Insight into the surface reaction mechanism of toluene oxidation over a composite $CeO_x/La_{1-x}Ce_xMnO_3$

catalyst using DRIFTS. Chem Eng Sci 259:117831
30. Jiang B, Xu K, Li J et al (2021) Effect of supports on plasma catalytic decomposition of toluene using in situ plasma DRIFTS. J Hazard Mater 405:124203
31. Fan J, Ning P, Song Z et al (2018) Mechanistic aspects of NH_3-SCR reaction over CeO_2/TiO_2-ZrO_2-SO_4^{2-} catalyst: In situ DRIFTS investigation. Chem Eng J 334:855–863
32. Chen L, Ren S, Jiang Y et al (2022) Effect of Mn and Ce oxides on low-temperature NH_3-SCR performance over blast furnace slag-derived zeolite X supported catalysts. Fuel 320:123969
33. Zhu X, Zhang L, Dong Y et al (2021) NO_2–NH_3 SCR over activated carbon: A combination of NH_4NO_3 formation and consumption. Energy Fuels 35:6167–6178
34. Wang Z, Zhou X, Wang G et al (2024) High-performance Ir_1/CeO_2 single-atom catalyst for the oxidation of toluene. Inorg Chem 63:7241–7254
35. Li X, Lai C, Zhang Y et al (2024) Bifunctional catalysts V-Cu/TiO_2 for selective catalytic reduction of NOx and CO oxidation under oxygen-rich conditions. Mol Catal 569:114574
36. Zhang Y, Yue X, Huang T et al (2018) In Situ DRIFTS Studies of NH_3-SCR mechanism over V_2O_5-CeO_2/TiO_2-ZrO_2 catalysts for selective catalytic reduction of NOx. Materials 11:1307
37. Bahamon D, Khalil M, Belabbes A et al (2021) A DFT study of the adsorption energy and electronic interactions of the SO_2 molecule on a CoP hydrotreating catalyst. Rsc Adv 11:2947–2957
38. Salih HS, Kareem MT, Jibrael KJ (2024) Influence of electron-donating groups on the aniline oxidative coupling reaction with promethazine: a comprehensive experimental and theoretical investigation. React Kinet Mech Catal 137:3265–3296

Figures

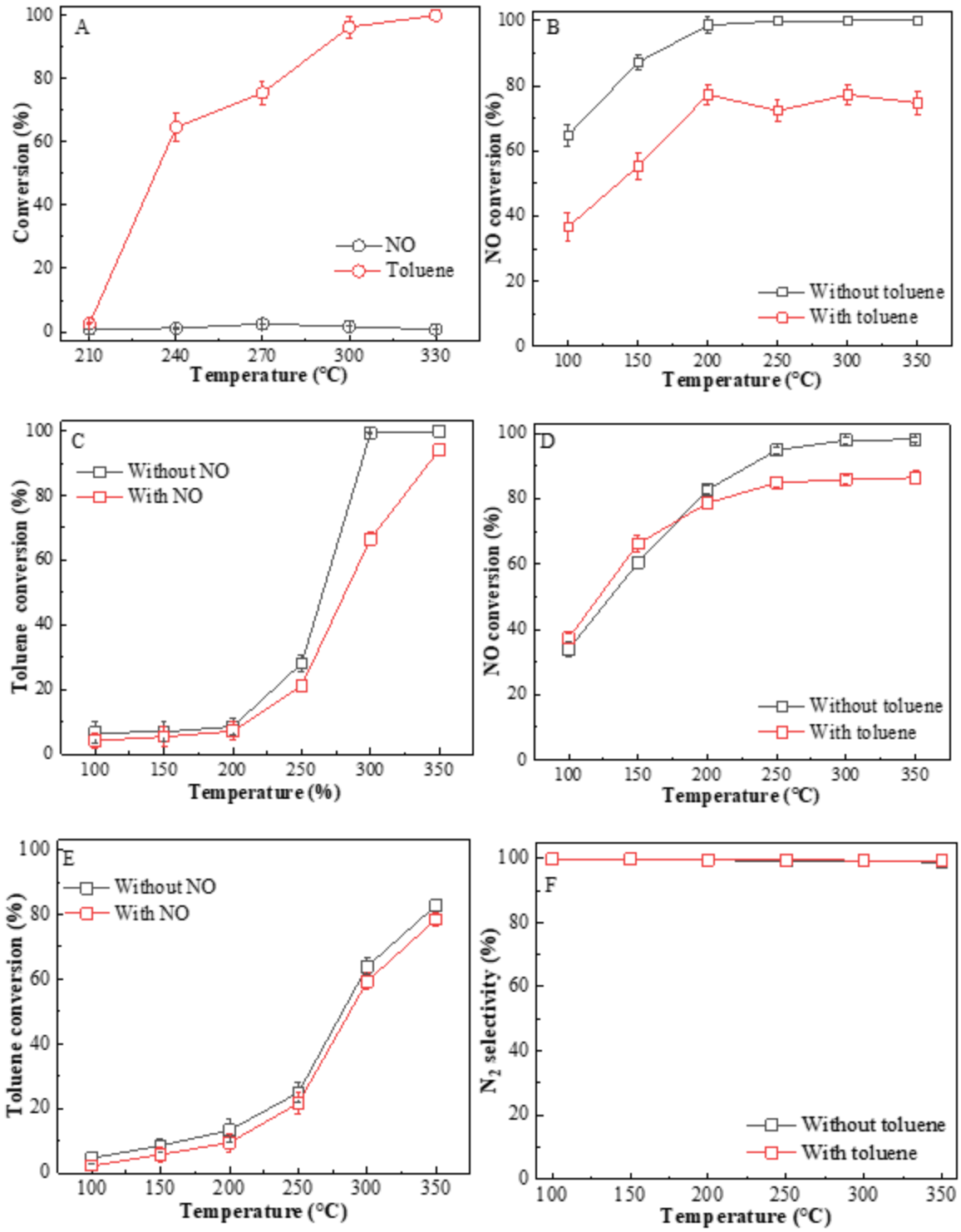


Figure 1

NO and toluene conversions under 500-ppm toluene, 500-ppm NO, and 10% O_2 by V/TiO_2 (**A**); Influence of 500-ppm toluene (**B**) and 500-ppm NO (**C**) on SCR and toluene catalytic oxidation, respectively, by V/TiO_2. NO_X conversion (**D**), toluene conversion (**E**), and N_2 selectivity (**F**) under 500-ppm toluene, 500-ppm NO, 500-ppm NH_3, and 10% O_2 by CeV/TiO_2.

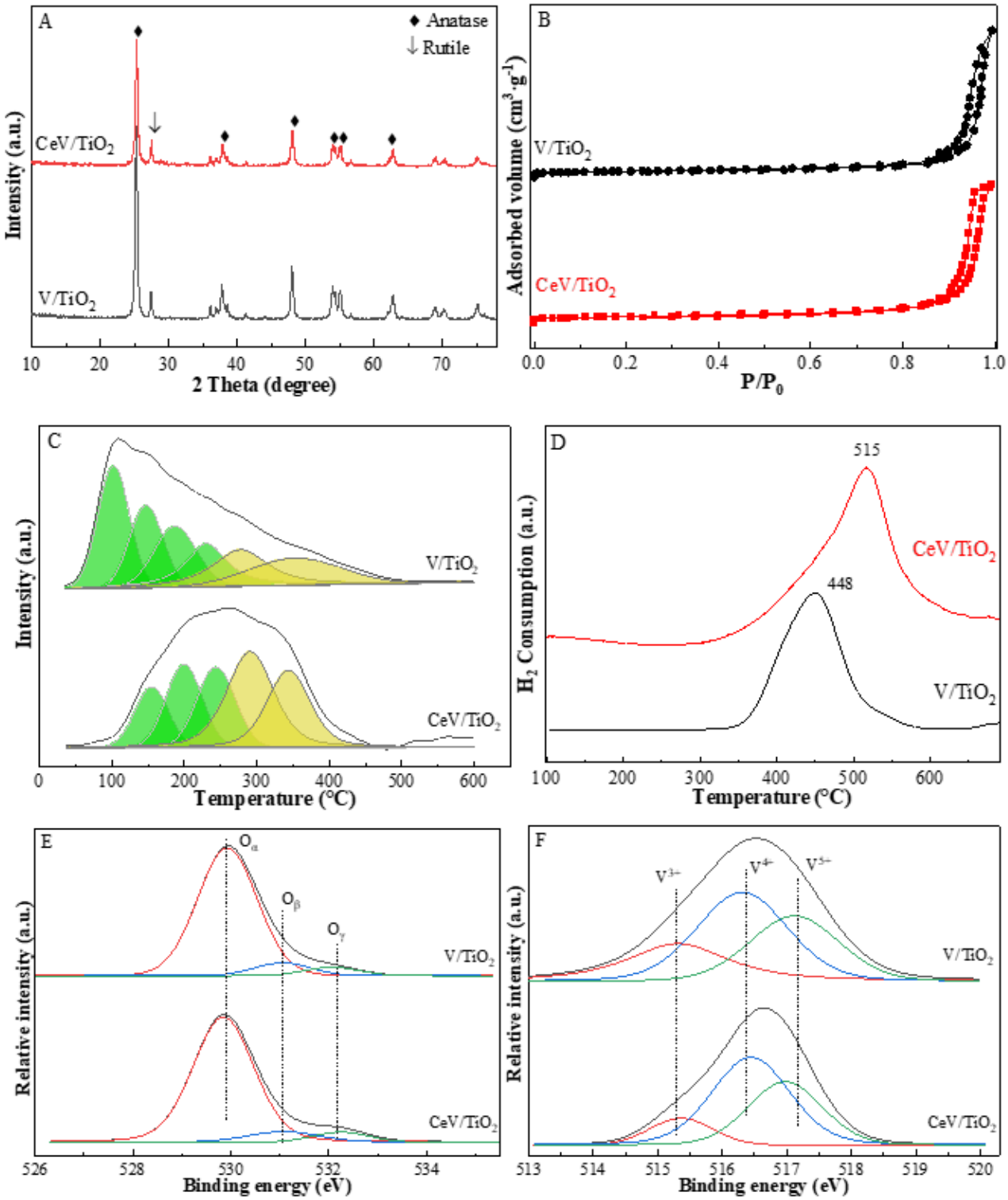


Figure 2

XRD (**A**), N_2 adsorption–desorption isotherms (**B**), NH_3-TPD (**C**), H_2-TPR (**D**), XPS O 1s (**E**), and XPS V 2p (**F**) of V/TiO_2 and CeV/TiO_2.

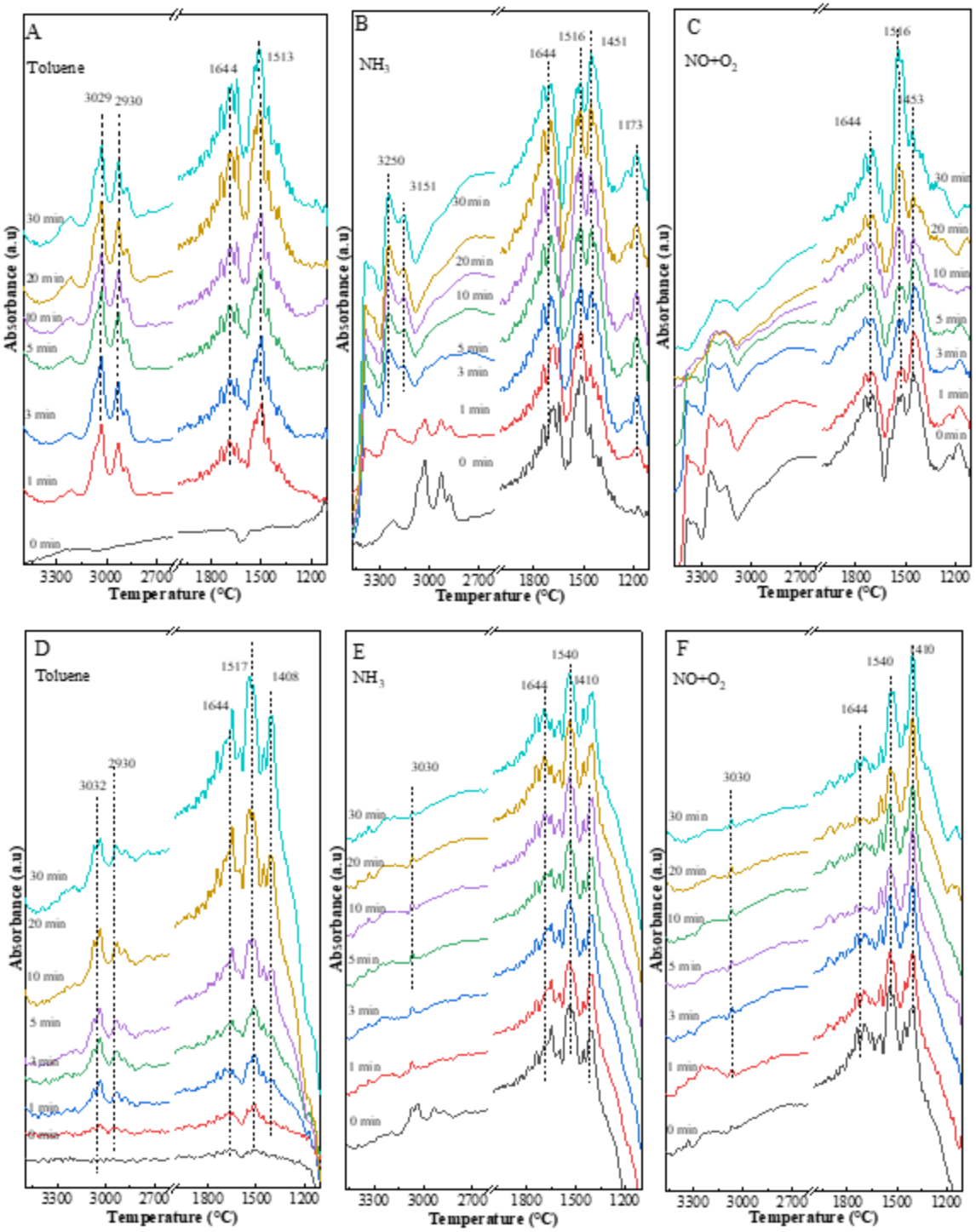


Figure 3

DRIFTs of toluene (**A**) — NH_3 (**B**) — $NO+O_2$ (**C**) adsorptions on CeV/TiO_2 at 250°C; DRIFTs of toluene (**D**) — NH_3 (**E**) — $NO+O_2$ (**F**) adsorptions on V/TiO_2 at 250°C.

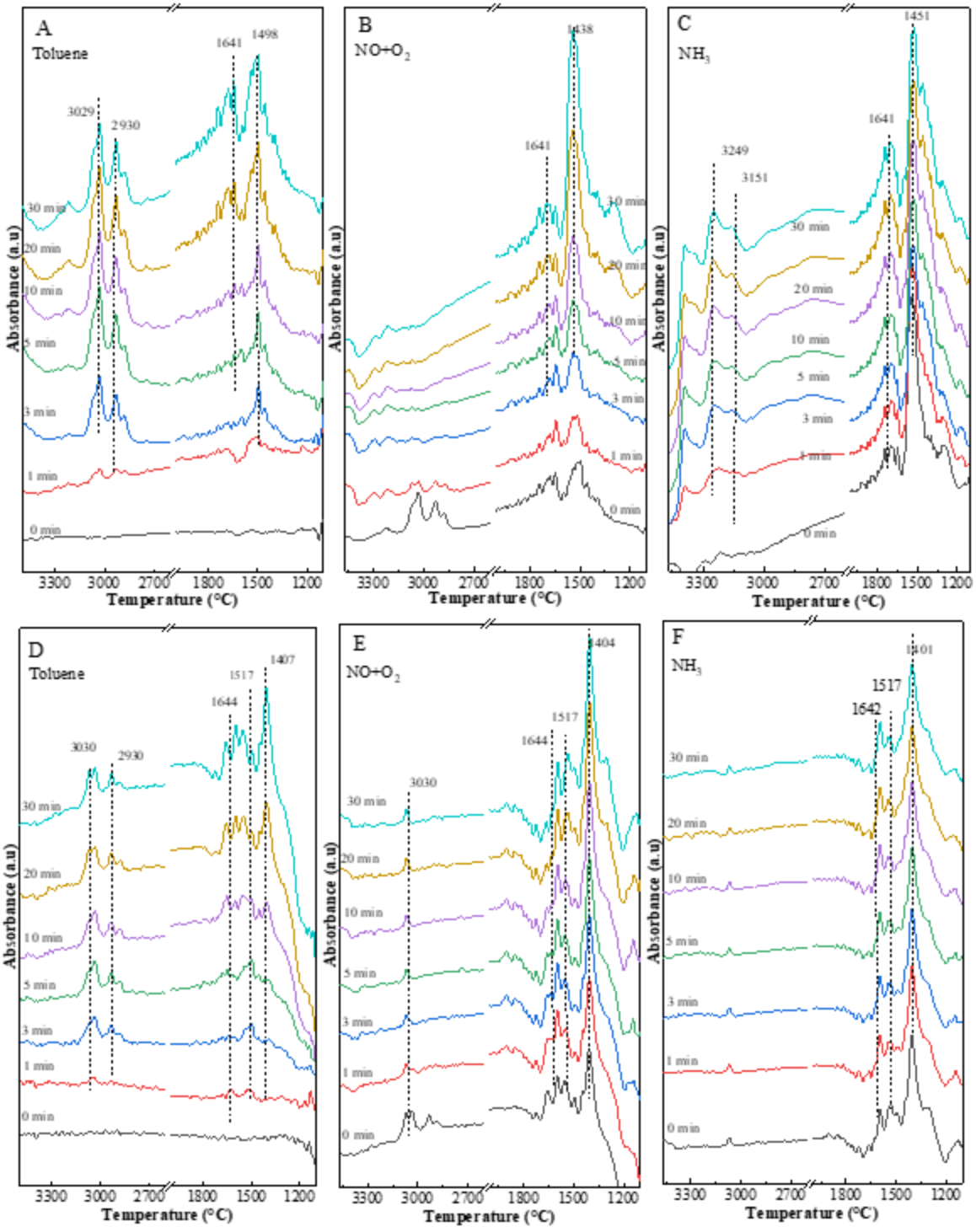


Figure 4

DRIFTs of toluene (**A**) — $NO+O_2$ (**B**) — NH_3 (**C**) adsorptions on CeV/TiO_2 at 250°C; DRIFTs of toluene (**D**) — $NO+O_2$ (**E**) — NH_3 (**F**) adsorptions on V/TiO_2 at 250°C.

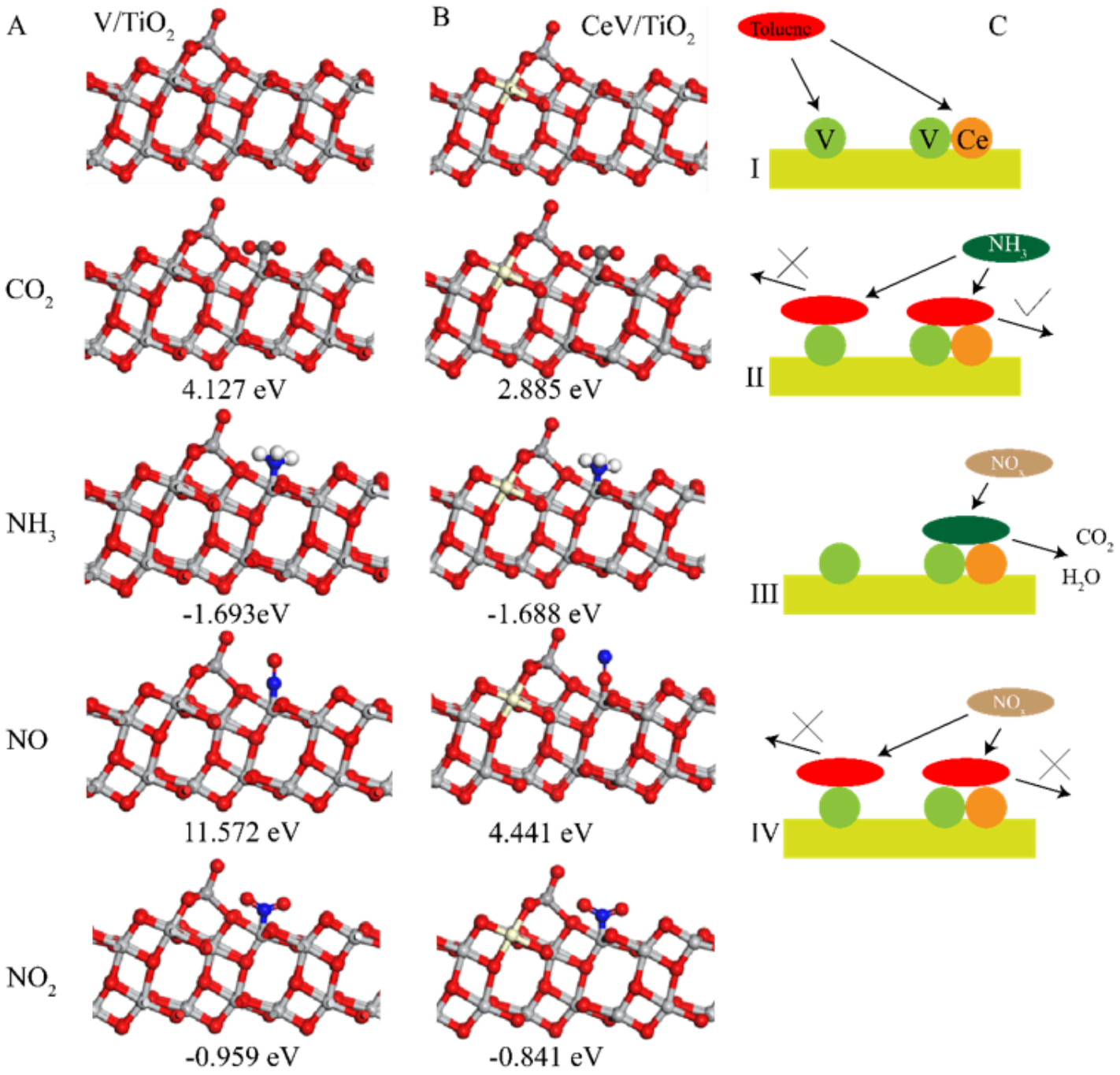


Figure 5

Adsorption energies of different gases on V/TiO_2 (**A**) and CeV/TiO_2 (**B**). Mechanism of stable simultaneous removal of toluene and NO (**C**).

Supplementary Files

This is a list of supplementary files associated with this preprint. Click to download.

- SupportingInformation.docx

- GA.png